Catalytic activity and some related spectral features of yttria-stabilised cubic sulfated zirconia

C. Morterra [a,*], G. Cerrato [a], G. Meligrana [a], M. Signoretto [b], F. Pinna [b] and G. Strukul [b]

[a] *Department of Chemistry IFM, Universiy of Turin, Via P. Giuria 7, I-10125 Turin, Italy*
[b] *Department of Chemistry, University of Venice, Calle Larga S. Marta 2137, I-30123 Venice, Italy*

Received 9 January 2001; accepted 15 March 2001

Cubic sulfated zirconia (c-SZ) was prepared by sulfating phase-stabilised c-ZrO_2, and its properties are compared with those of tetragonal (t-SZ) and monoclinic (m-SZ) systems. ZrO_2 crystalline phases have been identified by XRD and, far more efficiently, by Raman spectroscopy. c-SZ exhibits better catalytic activity (*n*-butane isomerization at 423 K) than t-SZ, whereas m-SZ is virtually inactive. The better activity of c-SZ is not ascribable to changes of surface functionalities, but probably derives from a better stabilization of the high symmetry crystalline form (i.e., from a more favourable distribution of surface sulfates among regular and defective crystal terminations).

KEY WORDS: cubic zirconia; sulfated zirconia (SZ) catalysts; *n*-butane isomerisation; surface acidity of SZ catalysts; IR spectra of adsorbed pyridine

1. Introduction

Since their first discovery, catalytic systems based on sulfated zirconia (SZ) have attracted extensive attention, due to their apparently unusual acidic properties and their high activity in light *n*-alkanes conversion in mild conditions. In recent years, much work has been devoted to studies of preparation, surface characterization, and possible applications of these catalytic materials. In particular, it has been shown that acidic and catalytic properties of SZ-based catalysts depend on a very high number of preparative parameters, among which particularly important are sulfation procedure [1], calcination temperature, and activation conditions [2]. It has been also reported that, in general terms, a stable tetragonal zirconia phase (t-ZrO_2) seems to be a necessary structural condition to obtain SZ systems catalytically active in the isomerisation reaction of light *n*-alkanes. Only in very few cases was it claimed that sulfation of the thermodynamically more stable monoclinic zirconia phase (m-ZrO_2) may lead to catalytic performances comparable to those of sulfated t-ZrO_2 (e.g., see [3]). The more favourable condition of tetragonal SZ (t-SZ) can be met by either calcining at $T \geqslant 750$ K a pre-sulfated amorphous hydrous zirconia precursor [4], or by direct sulfation of a phase-stabilized crystalline t-ZrO_2 precursor [5]. Recently, Bedilo et al. [6] reported the preparation of a monoclinic SZ (m-SZ) and of cubic SZ (c-SZ) catalysts obtained by direct sulfation of a crystalline m-ZrO_2 and of several Ca-stabilised cubic zirconia (c-ZrO_2) preparations, respectively. These catalysts turned out to be moderately active in the isomerization of *n*-alkanes, and the authors claimed that this was the first example of active SZ catalysts obtained starting from crystalline ZrO_2 precursors; while this is not entirely true for m-SZ, it is certainly true for the c-SZ systems.

It is known that, in ordinary temperature conditions, stable t- and c-ZrO_2 phases can be only obtained by incorporating in a zirconia matrix some metal oxides (e.g., Y_2O_3, CaO) to form solid solutions [7]. The present contribution aims to demonstrate that direct sulfation of a Y_2O_3-stabilised crystalline c-ZrO_2 phase leads to catalytically active SZ systems, as in the case of phase-stabilised t-ZrO_2 preparations. The very low activity, if any, of SZ systems obtained by sulfation of phase-pure m-ZrO_2 systems will be also confirmed.

2. Experimental

2.1. Catalysts preparation

Single-phase c-ZrO_2 was obtained by the incorporation of 11 mol% of Y_2O_3 into ZrO_2, to form a high-loading solid solution. The sample was prepared by controlled coprecipitation from aqueous solutions of $ZrOCl_2{\cdot}8H_2O$ and $YCl_3{\cdot}6H_2O$, carried out at room temperature and at constant pH (pH = 10). The precipitate was aged in the mother liquor for 90 h, filtrated and washed from chloride ions. The parent hydrogel (hereafter termed TO11) was then redispersed in ethanol and dried in air at 383 K for 20 h. The dry powdery material was then calcined in air at 923 K (leading to the crystalline system termed $TO11_{923}$), sulfated with $(NH_4)_2SO_4$ (8 wt% with respect to the oxide), and eventually calcined again at 923 K, yielding the catalytic system termed $TO11_{923}$S-923.

Single-phase t-ZrO_2 (tetragonal) and m-ZrO_2 (monoclinic) systems were also prepared for comparison purposes:

* To whom correspondence should be addressed.

1011-372X/01/0500-0113$19.50/0

(i) t-ZrO_2 was obtained by the same experimental procedure reported above for the cubic modification, but using 3 mol% Y_2O_3, and ageing the precipitate in the mother liquor for 65 h. The hydrogel (termed TO3) was then dried, calcined in air at 923 K, sulfated and calcined again (following the same steps reported above for the TO11 sample). The second and fourth operation lead to the formation of crystalline systems termed $TO3_{923}$ (phase-stabilised t-ZrO_2) and $TO3_{923}$S-923 (t-SZ), respectively. (ii) m-ZrO_2 was obtained by the room temperature hydrolysis of Zr-propoxide, followed by a calcination in air at $T \geqslant 730$ K, as reported in [8]. Of the various crystalline systems so obtained (termed ZRP_T), the oxide first fired at 923 K, and termed ZRP_{923}, was then sulfated and calcined at 923 K, yielding a SZ system hereafter referred to as ZRP_{923}S-923.

2.2. Sample analysis

The amount of sulfates was determined by ion chromatography [9].

Surface area and pore size information was obtained from N_2 adsorption/desorption isotherms at 77 K, using a Micromeritics ASAP 2010 analyzer. Prior to measurement, all samples were degassed to 1×10^{-3} Torr at 573 K for 4 h. Surface areas were calculated using the BET equation [10]. Mesopore size distributions were elaborated using the Barrett, Joyner and Halenda (BJH) method [10]. Assessments of microporosity were made from *t*-plot constructions, using the Harkins–Jura correlation [11] with t as a function of p/p_0.

FTIR spectra were obtained at 2 cm^{-1} resolution with a Bruker IFS 113v spectrophotometer equipped with MCT detector. The powdery samples were investigated in the form of thin layer depositions ($\sim$10 mg cm^{-2}) on a pure Si wafer. All samples were activated *in situ* at the chosen temperatures in quartz cells, equipped with KBr windows, connected to a conventional vacuum glass line capable of a residual pressure $<1 \times 10^{-5}$ Torr.

XRD patterns were obtained using a Philips PW 1810 powder diffractometer operating in a Bragg–Brentano geometry, equipped with a graphite crystal monochromator and using Cu K_α radiation.

Raman spectra were obtained at 4 cm^{-1} resolution using a FRA 106/RFS 100 FT Bruker spectrophotometer, equipped with a Nd/YAG laser (near-IR emission and variable power in the 0–300 mW range) and with a Ge detector (D418-S).

Catalytic activity was studied in a quartz flow reactor operating at atmospheric pressure and 423 K (*n*-butane : helium = 1 : 4) with a total space velocity = 720 h^{-1}. Prior to reaction, the catalysts (0.5 g) were activated *in situ* at 673 K in a dry air flow for 90 min, and then cooled to reaction temperature. Reactants and products were analysed on line by gas chromatography. Normalised activity is reported as moles per hour per unit surface area (m^2).

Table 1
Sulfate concentration and specific surface area of some ZrO_2 and SZ systems.

Sample	SO_4 (wt%)	n_{SO_4} (nm^{-2})	Surface area ($m^2\,g^{-1}$)
$TO3_{923}$	–	–	67
$TO11_{923}$	–	–	89
ZRP_{923}	–	–	47
$TO3_{923}$S-923	3.0	2.9	65
$TO11_{923}$S-923	4.0	3.9	75
ZRP_{923}S-923	2.2	2.8	39

3. Results and discussion

3.1. Physical features and structural data

The first calcination at 923 K brings about the crystallisation of the amorphous pure or mixed oxide precursors. As for the physical texture, all ZrO_2 samples so obtained are characterised by relatively high specific surface area (see table 1), the absence of microporosity, and the presence of a well-developed mesoporous texture (average pore sizes are in the 50–60 Å range for the c-ZrO_2 system, and in the 90–120 Å range for the other systems).

Data in table 1 also indicate that: (i) in non-sulfated systems, the incorporation of increasing amounts of yttrium cations to form solid solutions tends to increase the surface area; (ii) the sulfation/second-calcination process leaves almost unchanged the starting surface area of the t-ZrO_2 sample, whereas it reduces by some 16% the surface area of the c-ZrO_2 modification and by some 13% the surface area of the reference m-ZrO_2 sample.

The nature of the crystalline phases present both before and after the sulfation/second-calcination process was ascertained by X-ray diffraction (XRD) and by Raman spectroscopy.

3.1.1. XRD data

XRD patterns of some ZrO_2 and SZ systems are reported in figure 1. On the basis of well-known literature data [12], it can be stated that the $TO3_{923}$ specimen (curve (1) of figure 1) presents a diffractogram that is characteristic of the t-ZrO_2 modification, whereas the $TO11_{923}$ specimen (curve (2) of figure 1) presents a diffractogram that, as expected, is virtually indistinguishable from that of the t-ZrO_2 phase. In fact, the line broadening brought about by the small particle size of the present samples, prevents the line-splitting(s) that can sometimes indicate, in highly crystalline systems, the simultaneous presence of t- and c-ZrO_2 phases. In any event, the absence in the XRD pattern of the $TO11_{923}$ sample of a tiny reflection at $2\theta = 43.5°$, characteristic of the t-ZrO_2 phase (see the inset in figure 1), is at least compatible with the absence of any t-ZrO_2 component.

The m-ZrO_2 modification is known to possess a well characteristic XRD pattern [12b]. By comparing it with the XRD patterns of curves (1)–(4) of figure 1, it is possible to state that: (i) in the bulk of both $TO11_{923}$ and $TO3_{923}$ preparations, no XRD-detectable amounts of the m-ZrO_2

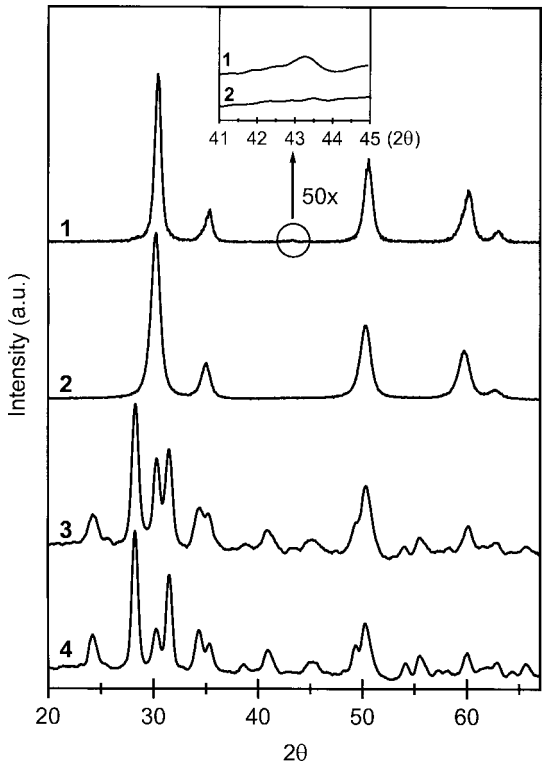

Figure 1. XRD diffractograms in the 20°–67° 2θ angles range of some ZrO_2 and SZ samples. (1) $TO3_{923}$, (2) $TO11_{923}$, (3) ZRP_{923} and (4) ZRP_{923}S-923. Inset: a blown-up (50×) segment of two XRD diffractograms in the 41°–45° range: (1) $TO3_{923}$ and (2) $TO11_{923}$.

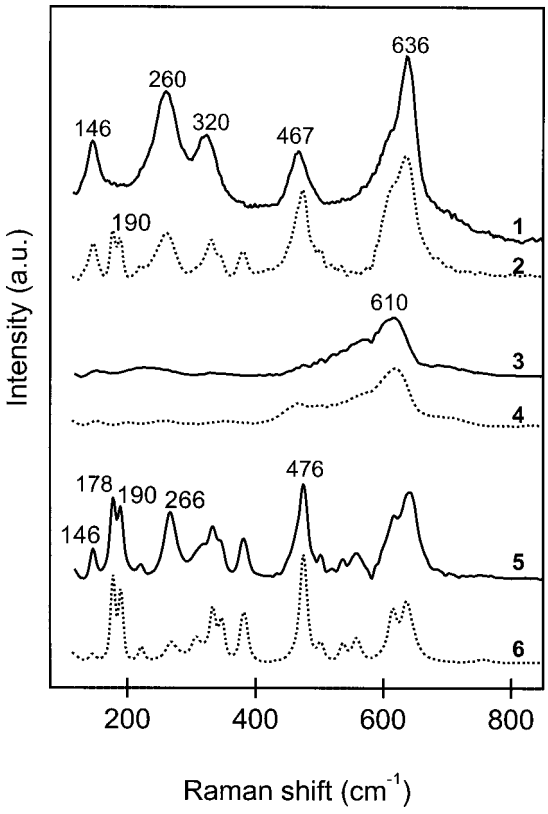

Figure 2. Laser Raman spectra of some ZrO_2 and SZ samples: (1) $TO3_{923}$, (2) $TO3_{923}$S-923, (3) $TO11_{923}$, (4) $TO11_{923}$S-923, (5) ZRP_{923} and (6) ZRP_{923}S-923.

modification are present; (ii) calcination at 923 K is insufficient to eliminate completely a minor t-ZrO_2 component from the ZRP preparation (in curve (3) of figure 1, the ratio t : m is 1 : 2.5 [13]), but the sulfation/second-calcination step tends to decrease drastically the residual t-ZrO_2 component present in the bulk of the ZRP_{923}-S preparation (in curve (4) of figure 1, t : m = 1 : 4).

3.1.2. Raman spectra

It is known that the XRD technique samples the bulk of the examined materials, whereas the Raman technique, being based on a scattering effect, samples preferentially the outermost layers of the examined materials. As we are mainly interested in the surface features of ZrO_2-based systems, Raman spectra were performed on pure and sulfated ZrO_2 powders. In particular both pure and sulfated systems were examined, as the presence of sulfate species may induce (surface) phase modifications. Some Raman spectra are reported in figure 2.

The t-ZrO_2 phase has been reported to possess several Raman bands in the 100–800 cm^{-1} range (145, 260, 320, 460 and 640 cm^{-1}) [14], among which the peaks at ∼145 and ∼260 cm^{-1} can be assumed as characteristic of the t-ZrO_2 phase. The latter bands, sharp and well resolved, are readily recognised in the pattern (1) of figure 2, due to the $TO3_{923}$ system, and remain the major components also on the corresponding sulfated/calcined system $TO3_{923}$S-923 (curve (2) of figure 2), although other well resolved peaks are observed on the latter sample. Among them, a sharp doublet centred at ∼180 cm^{-1}, ascribable to an m-ZrO_2 component (see below).

In the analytical spectral range above ∼100 cm^{-1}, the spectrum relative to the $TO11_{923}$ sample (reported as curve (3) in figure 2) presents one broad and ill-defined band, centred at ∼610 cm^{-1}, that can be assumed as characteristic of c-ZrO_2 [14b,14c]. After sulfation/second-calcination, the spectrum of $TO11_{923}$S (curve (4) of figure 2) is only marginally modified with respect to the starting c-ZrO_2 system: a shallow band is sometimes observed at ∼470 cm^{-1} that could be possibly ascribed to very minor amounts of a t-ZrO_2 component. But since no comparable (or stronger) bands are observed at ∼260 cm^{-1} (i.e., where there is the strongest and most typical Raman peak of t-ZrO_2), it seems more probable that changes in the region around ∼470 cm^{-1} are due to changes of disorder in the oxygen sublattice of the Y_2O_3-stabilised system. In fact, all the spectral features in the 450–580 cm^{-1} range of c-ZrO_2 have been demonstrated to be due to disorder-induced scattering [14c].

As for the m-ZrO_2 modification, a sharp doublet at ∼178 and ∼190 cm^{-1} and a sharp peak at ∼476 cm^{-1} can be assumed as highly sensitive analytical marks of the monoclinic phase (see [14]). The spectral patterns (5)–(6) of figure 2 present clear evidence of these spectral components, characteristic of the m-ZrO_2 phase. Moreover, the system ZRP_{923} (curve (5) of figure 2) exhibits appreciable spectral

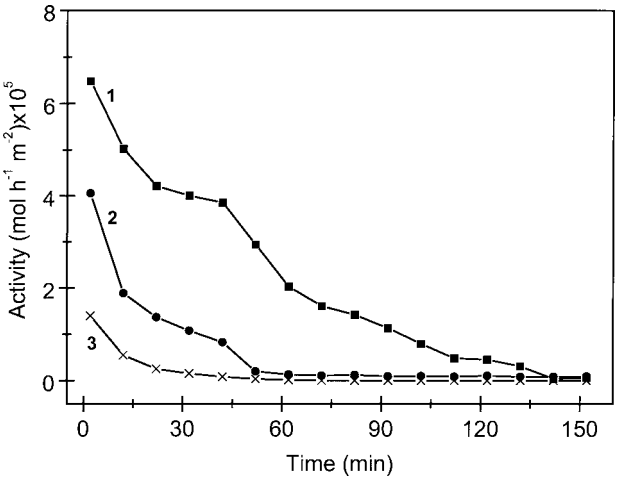

Figure 3. Normalised *n*-butane isomerisation activity at 423 K in He as a function of time on stream for different SZ systems: (1) $TO11_{923}$S-923, (2) $TO3_{923}$S-923 and (3) ZRP_{923}S-923.

components at ∼150 and ∼265 cm^{-1}, ascribable to a non-negligible fraction of t-ZrO_2, whereas on the corresponding sulfated/calcined ZRP_{923}S-923 system (curve (6) of figure 2) these spectral features have drastically decreased.

The data of figure 2 thus indicate that: (i) Raman spectroscopy is a highly sensitive technique in distinguishing, in a given sample, the presence/absence of the various ZrO_2 modifications; (ii) no spectroscopically detectable amounts of m-ZrO_2 are contained in (the outer layers of) $TO11_{923}$, $TO11_{923}$S-923 and $TO3_{923}$ samples, whereas in (the outer layers of) $TO3_{923}$S-923 specimens an m-ZrO_2 component is not negligible; (iii) a calcination temperature of 923 K is not sufficient to eliminate some of the t-ZrO_2 phase from the ZRP_T preparations, confirming the XRD data mentioned above, but the sulfation/second-calcination process tends to reduce drastically the residual t-ZrO_2 component.

3.2. Catalytic properties

Figure 3 reports the catalytic activity, as a function of time on stream, in the isomerization of *n*-butane at 473 K for the cubic, tetragonal, and monoclinic catalysts calcined, after sulfation, at 923 K and activated in a dry air flow at 673 K.

During the reaction, a fast initial activity decay can be observed in all systems, due to a partial deactivation process that is probably related to the formation of oligomeric species on the active sites. This initial deactivation process is not irreversible, and the activity can be completely restored by reactivating the various catalysts in dry air at 673 K, as previously reported for other SZ systems [15].

Among the samples calcined at 923 K, the c-SZ sample exhibits the best catalytic activity (see curve (1) in figure 3), while the monoclinic one (m-SZ), becomes (almost) completely inactive after the first (∼20 min) fast deactivation decay mentioned above (curve (3) in figure 3). This last result clearly contradicts the unusual findings reported by Stichert et al. [3] and Bedilo et al. [6] and confirms that, in general terms, m-SZ systems are hardly active at all, as reported in most literature data (e.g., see [5,16,17]).

Catalytic activity data not reported in figure 3 indicate that c-SZ systems calcined, after sulfation, at temperatures lower than 923 K are far less active and, if the second-calcination temperature is as low as 673 K, are virtually completely inactive. This behaviour is very similar to that exhibited, in similar conditions, by t-SZ catalysts [2]. Also the explanation is the same as previously given for the t-SZ systems: catalytic activity is induced by the second-calcination step, in that the actual role played by the calcination step is the selective elimination of sulfates from some specific (defective) terminations of the zirconia crystallites belonging to (one of) the high-symmetry crystal phases.

3.3. IR spectroscopic features

The higher catalytic activity exhibited by c-SZ catalysts is most interesting, and the next sections will be devoted to understanding if this higher activity can be somehow related to any observable difference of surface properties.

In order to test some of the surface properties (like, for instance, surface functionalities and/or surface acidity) of c-SZ and related systems, *in situ* FTIR spectroscopy of both pure powdery catalysts and of probe molecules adsorbed thereon has been resorted to.

3.3.1. Surface hydroxyls

It has been reported that the OH stretching (ν_{OH}) spectral region of activated zirconia-based systems usually contains two high-ν bands ascribable to OH groups free from H-bonding: a higher-ν component (∼3770 cm^{-1}) is due to the ν_{OH} mode of terminal (mono-coordinated) OH species, whereas a lower-ν component (∼3680 cm^{-1}) is due to the ν_{OH} mode of bridged (either bi- or tri-coordinated) OH species (e.g., see [8,18]).

Figure 4(a) reports the spectral profile in the ν_{OH} region of some systems of interest, activated *in vacuo* at 673 K, i.e., brought to a medium-high dehydration stage comparable to that usually attained by working SZ catalysts, before the catalytic tests. It is noted that OH groups are present at the surface of all systems examined, although the actual OH spectral profile varies appreciably. In the pure cubic $TO11_{923}$ system (curve (1) of figure 4(a)) the high-ν terminal OH species is virtually absent, whereas in the case of the pure tetragonal $TO3_{923}$ system (curve (3) of figure 4(a)) the high-ν terminal OH species is very scarce but not absent, and the sulfate-free (mostly) monoclinic system ZRP_{923} (curve (4) of figure 4(a)) exhibits at ∼3775 cm^{-1} a strong OH component (its intensity is comparable to that of the bridging OH species, centred at ∼3680 cm^{-1}). Curve (2) of figure 4(a), relative to the c-SZ system $TO11_{923}$S-923, indicates that the sulfation–calcination process brought about some appreciable physical/chemical changes in the termination of the c-ZrO_2 crystallites: a terminal OH component is now present at ∼3760 cm^{-1} (although still very weak in respect to the pure m-ZrO_2 modification), and the band due

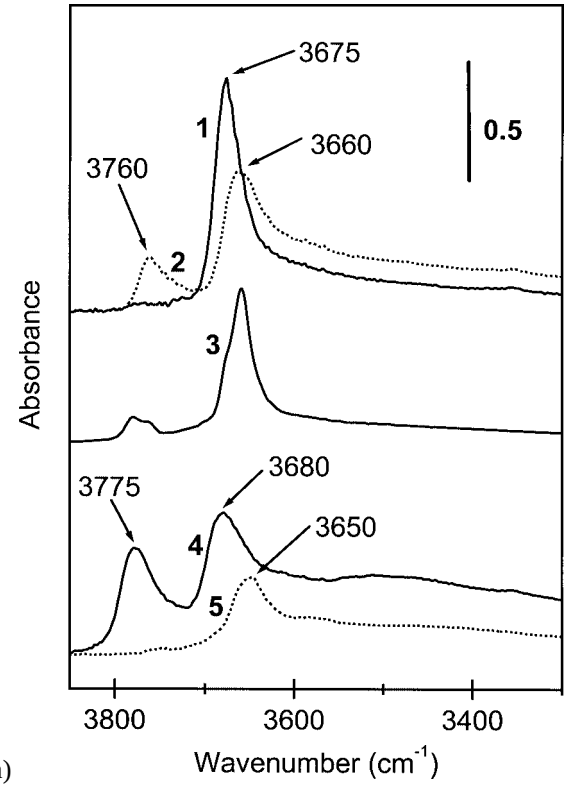

(a)

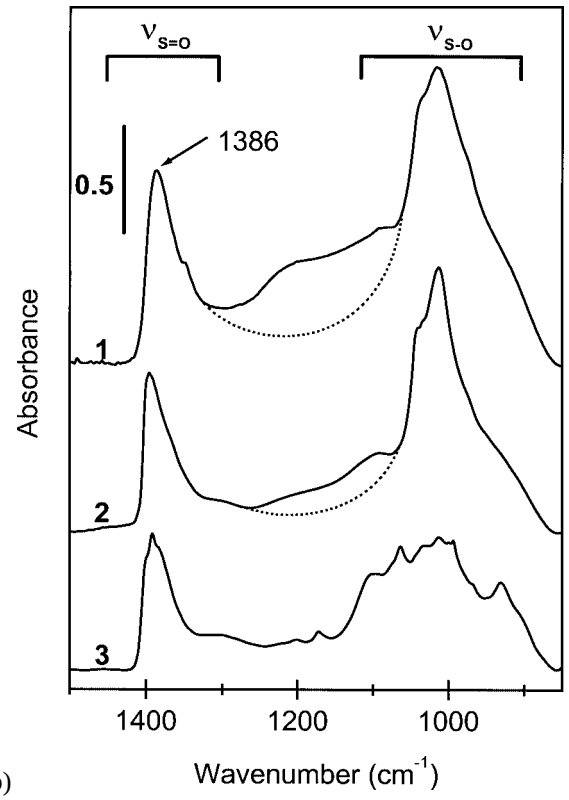

(b)

Figure 4. (a) Absorbance FTIR spectra in the ν_{OH} spectral region of some ZrO_2 and SZ samples, after activation *in vacuo* at 673 K. (1) $TO11_{923}$, (2) $TO11_{923}$S-923, (3) $TO3_{923}$, (4) ZRP_{923} and (5) ZRP_{923}S-923. (b) Absorbance FTIR spectra in the sulfate stretchings spectral region of some SZ samples, after activation *in vacuo* at 673 K. (1) $TO11_{923}$S-923, (2) $TO3_{923}$S-923 and (3) ZRP_{923}S-923.

to bridging OH species is now definitely weaker and located at a somewhat lower wavenumber ($\sim$3660 cm^{-1}). The latter effect is thought to be a consequence of surface inductive effects, i.e., of the presence at the surface of charge-withdrawing sulfate groups. Upon sulfation, the behaviour of the t-ZrO_2 modification (not shown) is quite similar to that of the cubic one: there is moderate increase of the high-ν terminal OH component, and a downwards shift of the component due to bridging OH species.

Upon sulfation, the behaviour of the m-ZrO_2 modification turns out to be very different. On ZRP_{923}S-923, after sulfation the high-ν OH component (terminal OH groups) is completely absent indicating that, in m-ZrO_2, the terminal OH species possess a definitely more basic character (and are therefore completely eliminated by the acidic sulfate groups). As for the low-ν OH band, due to bridging OH species, also on m-SZ after sulfation the band is weaker (i.e., less OH groups of this type are present, due to the coverage of large fractions of the surface by sulfate groups), and is located at lower wavenumbers, due to inductive effects brought about by nearby sulfate species.

The spectra of surface OH species thus indicate a fairly similar behaviour of the two high-symmetry crystal modifications, and a rather different behaviour of the low-symmetry monoclinic phase.

3.3.2. Surface sulfates

The spectral features of sulfate groups at the surface of the $TO11_{923}$S-923 sample (c-SZ), activated *in vacuo* at 673 K, are reported in curve (1) of figure 4(b). The spectrum shows that the $\nu_{S=O}$ band is single (though rather asymmetric on the low-ν side) and located at very high wavenumber ($\sim$1400 cm^{-1}), and that the $\nu_{S=O}$ and ν_{S-O} modes present a large spectral separation. These spectral features are typical of highly covalent sulfates [19,20], and similar to what has been observed in the case of organic sulfates. Moreover, these spectral features (and, in particular, the large spectral separation between $\nu_{S=O}$ and ν_{S-O} modes) are typically observed with all catalytically active SZ systems. In fact, a very similar two-peaks spectral profile is observed in the case of the catalytically active $TO3_{932}$S-923 system (t-SZ) activated in the same conditions (see curve (2) in figure 4(b)), whereas the spectral profile of the virtually (inactive) monoclinic ZRP_{923}S-923 system, shown in curve (3) of figure 4(b), is very different, as already reported elsewhere [5,9].

In the case of the $TO11_{923}$S-923 system, strong absorptions in the 1300–1100 cm^{-1} region, usually ascribed to complex poly-sulfate surface species, are compatible with the large S contents retained by this specimen after the calcination step.

The spectra of surface sulfates confirm a close similarity between cubic and tetragonal zirconia modifications, and indicate that there is a large difference between the two high-symmetry phases and the monoclinic one. Moreover, the spectral profile of surface sulfates, after a medium-high temperature activation, confirms to represent a valuable

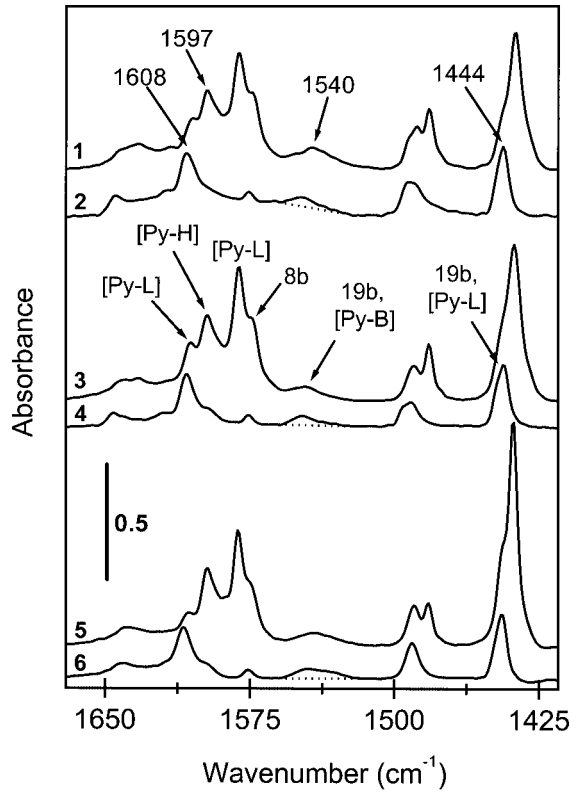

Figure 5. Absorbance FTIR spectra in the analytical ring-stretching region of py adsorbed on various SZ catalysts activated *in vacuo* at 673 K: (1) $TO11_{923}S$-923, $P_{py} = \sim 5$ Torr, (2) $TO11_{923}S$-923, excess py evacuated for 15 min, (3) $TO3_{923}S$-923, $P_{py} = \sim 5$ Torr, (4) $TO3_{923}S$-923, excess py evacuated for 15 min, (5) $ZRP_{923}S$-923, $P_{py} = \sim 5$ Torr and (6) $ZRP_{923}S$-923, excess py evacuated for 15 min. The symbol [pyL] stands for Lewis-coordinated py, [py-B] for (Brønsted) pyridinium ions, and [py-H] for H-bonded py species.

probe for the catalytic activity of SZ systems in the low-temperature isomerisation of light *n*-alkanes.

3.3.3. The adsorption of pyridine

To find out if the differences of catalytic activity exhibited by the various SZ materials can derive from their acidic character, some pyridine (py) adsorption experiments were carried out. In fact, it is known that the presence of Brønsted and/or Lewis acidity can be easily evidenced by py adsorption/desorption at RT [21], in that well-resolved specific IR bands ascribable either to Lewis acid sites (for instance, the 19b mode of [py-L] species, $\sim$1445 cm^{-1}) or to Brønsted acid sites (the 19b mode of [py-B] species, $\sim$1540 cm^{-1}) may be singled out in the IR spectrum.

IR spectra of py adsorbed/desorbed at ambient temperature on sulfated-and-calcined TO11, TO3 and ZRP systems activated in comparable conditions are reported in figure 5. The spectra indicate that: (i) on all SZ preparations considered, both Lewis and Brønsted acidic sites are present. This is not unexpected, as it is known that surface sulfates may induce Brønsted acidity in oxidic systems that, otherwise, do not possess any protonic acidic activity; (ii) when the spectra are run in the presence of an excess py (see curves (1), (3) and (5) in figure 5), several py species can be evidenced on the basis of their analytical IR bands (symbols on the spectra and in the figure caption indicate the py species). In particular, a strong band centred at $\sim$1597 cm^{-1} is ascribable to the 8a mode of py H-bonded to some of the residual surface OH species ([py-H]) and/or to py coordinated to surface Lewis acid centres weaker than coordinatively unsaturated (cus) Zr^{4+} cationic sites (the relevant 8a py mode absorbs typically at $\sim$1610 cm^{-1}). In the case of TO11 specimens and, to some minor extent, of TO3 specimens one can think of the possible Lewis coordination of py to surface cus Y^{3+} sites. But the spectra run after prolonged evacuation of the excess py (see curves (2), (4) and (6) in figure 5) indicate that very little of the 8a py band at $\sim$1600 cm^{-1} remains on the three samples and, more important, with virtually the same intensity on the three samples. This definitely rules out the possibility that cus Y^{3+} sites contribute to an appreciable extent to the $\sim$1600 cm^{-1} band, as no yttrium is contained in the monoclinic ZRP specimens. It is so deduced that, even in the presence of large amounts of the basic Y_2O_3 oxide, the surface acidic properties of phase-stabilised SZ remain virtually unchanged.

Table 2
Lewis-to-Brønsted ratio relative to py adsorption/evacuation on SZ samples, activated at different temperatures.

Sample	L/B ratio	
	Act. at $\sim$300 K	Act. at 673 K
$TO3_{923}S$-923	1.57	2.70
$TO11_{923}S$-923	1.60	3.01
$ZRP_{923}S$-923	1.53	3.06

Finally, in order to understand if the widely different catalytic properties of the three SZ systems examined may reside in a different distribution of the surface acidic properties, the Lewis-to-Brønsted (L/B) sites ratio has been evaluated from spectroscopic data relative to py adsorption/evacuation at ambient temperature. L/B ratios, some of which are reported in table 2, are largely approximate (and thus merely indicative) because: (i) it is assumed that the Beer–Lambert law applies to heterogeneous systems and this assumption is, most often, not so realistic (e.g., see [22,23]); (ii) the molar absorption coefficients of the analytical bands of adsorbed py, first calculated for zeolitic systems [24], are assumed to remain constant on passing from one oxidic system to another; (iii) an appreciable overestimation of the Lewis acidity content, typical of SZ systems and due to a py/sulfates ligand displacement effect [22], is neglected (as it is impossible to express it in quantitative terms). Data in table 2 indicate that the L/B ratios increase appreciably with activation temperature, and this is quite obvious as upon activation more cus cationic sites (Lewis acid centres) are created and less (Brønsted) acidic OH groups remain on/by surface sulfates. The increase of L/B ratios with increasing activation temperature is virtually the same on all SZ systems examined. The data of table 2 also indicate that the L/B ratio on the different catalysts vacuum activated at the highest temperature examined (and roughly corresponding to the flux activation carried out on working catalysts) is virtually

the same and, in particular, it is the same on the two systems (m-SZ and c-SZ) representing the two extremes in terms of catalytic performance. It is so deduced that the different catalytic behaviour exhibited by different SZ systems does not derive from a different distribution (in terms of aprotic and protonic acid centres) of the surface acidic features, and that a high L/B ratio (that is certainly a necessary condition for a good isomerisation catalytic activity [2]) is not a sufficient condition to give SZ catalysts a good catalytic activity.

4. Conclusions

(i) This work shows that catalytically active SZ systems can be obtained also by direct sulfation of crystalline ZrO_2 precursors, provided that the starting crystalline phase is the right one, i.e., one of the high-symmetry ZrO_2 modifications. Needless to say, the mere sulfation is insufficient to yield an active SZ catalyst, but the sulfation step must be followed by a proper calcination process and by an activation treatment, as reported in the literature for SZ catalysts deriving from amorphous precursors.

(ii) High amounts (11 mol%) of Y_2O_3 added to ZrO_2 have been confirmed to stabilise a cubic ZrO_2 phase. The cubic phase turns out to be quite pure, as shown by the combined use of X-ray diffraction and, more important, of Raman spectroscopy. The large amounts of Y_2O_3 added, necessary to stabilise the cubic solid solution, do not alter to an appreciable extent any of the main surface features of the system, among which the surface OH composition and the surface acidity/basicity.

(iii) The catalytic activity of the c-SZ system turns out to be by far the highest one among those of the three ZrO_2 phases examined. This increase of activity is not ascribable to dramatic changes of surface functionalities like OH groups and/or sulfate species (in particular, these functionalities are fairly similar in the case of t-SZ and c-SZ), nor to a change of either the number or the distribution of protonic and aprotic surface acidic centres. The enhanced catalytic activity ought to be sought for, probably, in a better surface stabilisation of the high-symmetry form(s) possibly leading to a sharper difference of distribution of surface sulfates between regular low-index crystal terminations (where sulfates remain after the calcination step, and carry the Brønsted acid functionality) and defective crystal terminations (wherefrom sulfates are eliminated during the calcination step, and strong Lewis acidity can develop during the catalyst activation step).

Acknowledgement

Raman spectra were run by Dr. A. Frache (Università del Piemonte Orientale), and his contribution to this work is gratefully acknowledged. This work was partly financed by the Italian Ministero dell'Università e della Ricerca Scientifica (MURST), project COFIN 98, section 03.

References

[1] R.A. Comelli, C.R. Vera and J.M. Parera, J. Catal. 151 (1995) 96.
[2] C. Morterra, G. Cerrato and M. Signoretto, Catal. Lett. 41 (1996) 101.
[3] W. Stichert and F. Schüth, J. Catal. 174 (1998) 242.
[4] K. Arata, Adv. Catal. 37 (1990) 165.
[5] C. Morterra, G. Cerrato, F. Pinna and M. Signoretto, J. Catal. 157 (1995) 109.
[6] A.F. Bedilo, A.S. Ivanova, N.A. Pakhomov and A.M. Volodin, J. Mol. Catal. A 158 (2000) 409.
[7] (a) D. Steele and B.E.F. Fender, J. Phys. C 7 (1974) 1;
(b) H.G.J. Scott, J. Mater. Sci. 10 (1975) 1527.
[8] (a) M. Bensitel, O. Saur, J.-C. Lavalley and G. Mabilon, Mater. Chem. Phys. 17 (1987) 249;
(b) C. Morterra, R. Aschieri and M. Volante, Mater. Chem. Phys. 20 (1988) 539.
[9] C. Sarzanini, G. Sacchero, F. Pinna, M. Signoretto, G. Cerrato and C. Morterra, J. Mater. Chem. 5 (1995) 353.
[10] J.S. Gregg and K.S.W. Sing, Adsorption, *Surface Area and Porosity*, 2nd Ed. (Academic Press, London, 1982).
[11] W.D. Harkins and G.J. Jura, J. Am. Chem. Soc. 66 (1944) 811.
[12] JCPDS files: (a) c-ZrO_2: 27-997; (b) m-ZrO_2: 36-420; (c) t-ZrO_2: 24-1164.
[13] P.A. Evans, R. Stevens and J.G.P. Binner, Br. Ceram. Trans. J. 83 (1984) 39.
[14] (a) P.D.L. Mercera, J.G. van Ommen, E.B.M. Doesburg, A.J. Burgraaf and J.R.H. Ross, Appl. Catal. 57 (1990) 127;
(b) D.A. Ward and E.I. Ko, Chem. Mater. 5 (1993) 956;
(c) J. Cai, C. Raptis, Y.S. Raptis and E. Anastassakis, Phys. Rev. B 51 (1995) 201;
(d) T. Takashi, T. Tanaka, S. Takenaka, S. Yoshida, T. Onari, Y. Takahashi, T. Kosaka, S. Hasegawa and M. Kudo, J. Phys. Chem. B 103 (1999) 2385;
(e) K. Tomishige, Y. Ikeda, T. Sakaihori and K. Fujimoto, J. Catal. 192 (2000) 355.
[15] F. Pinna, M. Signoretto, G. Strukul, G. Cerrato and C. Morterra, Catal. Lett. 26 (1994) 339.
[16] D.A. Ward and E.I. Ko, J. Catal. 157 (1995) 321.
[17] D. Spielbauer, G.A.H. Mekhemer, M.I. Zaki and H. Knözinger, Catal. Lett. 40 (1996) 71.
[18] A.A. Tsyganenko and V.N. Filimonov, J. Mol. Struct. 19 (1973) 579.
[19] T. Yamaguchi, T. Jin and K. Tanabe, J. Phys. Chem. 90 (1986) 3148.
[20] M. Waquif, J. Bachelier, O. Saur and J.-C. Lavalley, J. Mol. Catal. 72 (1992) 127.
[21] E.P. Parry, J. Catal. 2 (1963) 371.
[22] C. Morterra and G. Cerrato, Phys. Chem. Chem. Phys. 1 (1999) 2825.
[23] C. Morterra, G. Magnacca and V. Bolis, Catal. Today, in press.
[24] C.A. Emeis, J. Catal. 141 (1993) 347.